



Research paper

EGCG inactivates a pore-forming toxin by promoting its oligomerization and decreasing its solvent-exposed hydrophobicity[☆]



Justus M. Gabriel^a, Thomas Tan^a, Dillon J. Rinauro^b, Claire M. Hsu^a, Caleb J. Buettner^a, Marshall Gilmer^a, Amrita Kaur^a, Tristan L. McKenzie^a, Martin Park^a, Sophie Cohen^a, Silvia Errico^{b,c}, Aidan K. Wright^a, Fabrizio Chiti^c, Michele Vendruscolo^b, Ryan Limbocker^{a,*}

^a Department of Chemistry and Life Science, United States Military Academy, West Point, NY 10996, USA

^b Centre for Misfolding Diseases, Yusuf Hamied Department of Chemistry, University of Cambridge, Cambridge, CB2 1EW, UK

^c Department of Experimental and Clinical Biomedical Sciences, Section of Biochemistry, University of Florence, Florence, Italy

ARTICLE INFO

Keywords:

Biotoxin neutralization
Membrane-toxin interactions
Pore-forming agents
Biotoxicology
Medical countermeasures
Biological threat agents

ABSTRACT

Natural proteinaceous pore-forming agents can bind and permeabilize cell membranes, leading to ion dyshomeostasis and cell death. In the search for antidotes that can protect cells from peptide toxins, we discovered that the polyphenol epigallocatechin gallate (EGCG) interacts directly with melittin from honeybee venom, resulting in the elimination of its binding to the cell membrane and toxicity by markedly lowering the extent of its solvent-exposed hydrophobicity and promoting its oligomerization into larger species. These physicochemical parameters have also been shown to play a key role in the binding to cells of misfolded protein oligomers in a host of neurodegenerative diseases, where oligomer-membrane binding and associated toxicity have been shown to correlate negatively with oligomer size and positively with solvent-exposed hydrophobicity. For melittin, which is not an amyloid-forming protein and has a very distinct mechanism of toxicity compared to misfolded oligomers, we find that the size-hydrophobicity-toxicity relationship also rationalizes the pharmacological attenuation of melittin toxicity by EGCG. These results highlight the importance of the physicochemical properties of pore forming agents in mediating their interactions with cell membranes and suggest a possible therapeutic approach based on compounds with a similar mechanism of action as EGCG.

1. Introduction

Cell homeostasis requires the maintenance of the integrity of the plasma membrane, which separates the intracellular and extracellular spaces and allows for the passage of essential molecules and ions into and out of the cell [1]. Pore-forming agents, misfolded protein oligomers, and other biotoxins can disrupt cell homeostasis by embedding themselves in the membrane, disrupting cellular receptors, and causing ion dyshomeostasis [2–4]. Many systemic and neurodegenerative diseases are also characterized by the inability of the cell to adequately repair or remove damaged cell membranes. Protecting cell membranes is therefore a possible strategy towards combatting these pathologies [1].

Biological threats have become a prevalent concern in modern

warfare [5]. Although very rarely used, they have the potential to cause catastrophic harm to Soldiers and civilians. Biological threat agents can include bacteria, viruses, fungi, other microorganisms and the toxins they produce that have the ability to adversely affect human health [6]. Many of these toxins occur in the natural environment, but have the potential to be weaponized, which emphasizes the need for methods to detect and counteract biological threat agents. Herein, we investigated pore-forming toxins (PFTs), a broad group of peptides and proteins that interact with the cell to form transmembrane pores, as a model biological threat agent.

PFTs can be classified as α or β based on the secondary structure composition of α -helices or β -barrels when embedded in the cell membrane [3,7–9]. Some PFTs target bacterial cells, and can be used as antimicrobial agents [4]. Other PFTs target the cell membrane of

[☆] Michele Vendruscolo is a founder of Wren Therapeutics. The views expressed herein are those of the authors and do not reflect the position of the United States Military Academy, the Department of the Army, or the Department of Defense.

* Corresponding author.

E-mail address: ryan.limbocker@westpoint.edu (R. Limbocker).

<https://doi.org/10.1016/j.cbi.2022.110307>

Received 18 September 2022; Received in revised form 2 December 2022; Accepted 14 December 2022

Available online 17 December 2022

0009-2797/Published by Elsevier B.V. This is an open access article under the CC BY license (<http://creativecommons.org/licenses/by/4.0/>).

eukaryotic cells and, in extreme cases, can be deadly to the organism [10]. General therapeutic approaches for these toxins include inhibition of pore formation and non-toxic PFT-based vaccines [3]. Pore formation can be inhibited by small molecules or engineered antibodies designed to target specific sites in the PFTs that are required for binding to the membrane or pore assembly [3]. Additionally, small molecules can target specific membrane receptors and prevent the recruitment of the PFTs to the membrane to impair pore formation, and vaccines against PFTs can create an immune response that sequesters the toxins in nanoparticles, therein preventing membrane binding [3].

In addition to exogenous agents like PFTs, other toxins can be produced endogenously within an organism through numerous pathways, including oligomers formed by endogenous proteins that fail to remain soluble and self-assemble to form misfolded protein oligomers [2]. In fact, over 50 protein misfolding diseases have been characterized by the misfolding and aggregation of proteins occurring either systemically or in the central nervous system [2]. Within these pathologies, Alzheimer's disease (AD) is the most common, and it is the leading cause of dementia worldwide [11]. In AD, monomers of the amyloid- β peptide ($A\beta$) misfold and form misfolded protein oligomers. A minority of oligomers act as primary nuclei and grow to become fibrillar species, which are a hallmark of AD [2,12]. It is now commonly accepted that oligomeric forms of $A\beta$, markedly more so than fibrillar aggregates, are the dominant cytotoxic species formed in the $A\beta$ aggregation process [13]. For several types of misfolded protein oligomers, cytotoxicity has been shown to positively correlate with membrane dysfunction, which can be further induced by oligomers of smaller size and a greater extent of solvent-exposed hydrophobicity [14]. The hydrophobicity of these oligomers allows them to embed in the lipid bilayer of the cell membrane and disrupt the function of the membrane [14]. Similarly, small size allows oligomers to diffuse more readily to the membrane and correlates with a higher propensity to bind to the phospholipid bilayer [15]. Tuning these physicochemical properties with molecular chaperones has been shown to mediate the interaction of oligomers with cell membranes and lower their toxicity [16–18].

In an effort to understand how PFTs damage cells and to concomitantly develop medical countermeasures that can attenuate their toxicity, we took advantage of the information gained from studies on misfolded protein oligomers and leveraged these key physicochemical properties to investigate the relationship between size, hydrophobicity, the extent of membrane binding, and cytotoxicity using melittin. Melittin, the active component of honeybee venom, is an extensively studied membrane-active peptide frequently used for its ability to model other pore-forming peptides [19–25]. It is a 2.85 kDa, amphipathic 26-residue peptide (Fig. 1a) that exhibits a random coil structure in solution and can adopt an α -helical secondary structure upon its interaction with membranes (Fig. 1b) [26,27]. Indeed, monomeric melittin readily interacts with phospholipids in the plasma membrane, acquiring

an α -helical structure that segregates its hydrophobic and hydrophilic residues [28]. The monomer consists of two helical segments joined by a coil containing a proline [26]. Melittin can interact with the cell membrane in either a parallel or perpendicular orientation, the former of which is innocuous and prevents the docking of additional peptides, whereas the latter alignment facilitates the formation of ~ 4.4 nm transmembrane pores [25]. These pores can induce membrane permeabilization, membrane disruption, ion dyshomeostasis, and cell death [25,27,29,30].

Our previous work has shown that claramine, a brain-permeable aminosterol, protects brain and kidney cells from two structurally diverse PFTs [31]. This was not found to be achieved by directly impacting their structures, but rather by changing the physicochemical properties of the plasma membrane in a way that prevented the docking of these toxins [31]. In addition to targeting the properties of the cell membrane, it is also possible to alleviate PFT-mediated cytotoxicity by targeting the toxin directly. To realize this strategy experimentally, we leveraged the polyphenol EGCG (Fig. 1c), a common catechin in green tea that is the ester of epigallocatechin and gallic acid. Various beneficial effects have been suggested for these tea catechins, and many have undergone or are currently undergoing clinical trials, including for the treatment of cancer, Alzheimer's and Parkinson's diseases, decreasing cholesterol absorption, increasing cardiovascular and metabolic health, and promoting weight loss and weight maintenance [32–38]. Tea catechins have been shown to have antioxidant, anti-inflammatory, and antiviral properties [39–42], and EGCG can cross the blood brain barrier [43]. Many of the aforementioned diseases are associated with a chronic inflammatory response and cellular oxidative stress. EGCG has previously been shown to inhibit key cytokines involved in the inflammatory response, such as tumor necrosis factor α (TNF- α) and interleukin-1 β (IL-1 β), and to modulate the diseases related to their chronic production [44,45]. In this report, we studied the protective effects of EGCG against melittin, a non-amyloid forming peptide with a distinct mechanism of action compared to misfolded protein oligomers, with a focus on the size-hydrophobicity-cytotoxicity relationship for protein-small molecule interactions.

2. Results

2.1. EGCG neutralizes the toxicity of melittin

We initially sought to measure the impact of increasing concentrations of EGCG on the toxicity induced by melittin (MEL). We therefore first conducted 3-(4,5-dimethylthiazol-2-yl)-2,5-diphenyltetrazolium bromide (MTT) cell viability assays on SH-SY5Y human neuroblastoma cells. Cells were exposed to melittin at a concentration of 2.5 μ M (equivalent to 7.1 μ g/mL) for 30 min in the absence and presence of increasing concentrations of EGCG ranging from 5 μ M to 100 μ M, corresponding to super-stoichiometric ratios of MEL:EGCG of 1:2 to 1:40, respectively. A well-defined dose-dependent decrease in melittin toxicity, or increase in cell viability, was observed with increasing concentrations of EGCG. Melittin caused a decrease in cell viability to $42 \pm 3\%$ relative to untreated cells (mean \pm standard error of the mean, s.e.m., $p < 0.001$) and cells treated with MEL and 40-fold excess of EGCG (100 μ M) had a viability of $88 \pm 5\%$ of untreated cells ($p < 0.001$ relative to MEL-treated cells without EGCG) (Fig. 2a). We have shown previously that the toxicity of melittin was similar whether SH-SY5Y cells were treated for 30 min or 24 h, and we therefore only studied the 30 min treatment time herein [31].

To gain a better understanding of the acute effects of EGCG in preventing the toxicity of melittin, we next assessed the extent of reactive oxygen species (ROS) production in SH-SY5Y cells. We explored lower concentrations of melittin in the more sensitive ROS assay because an increase in ROS production is usually more rapid and intense than a decrease of MTT reduction. Cells were seeded on glass coverslips and treated for 5 min with 0.33 μ M melittin in the absence or presence of

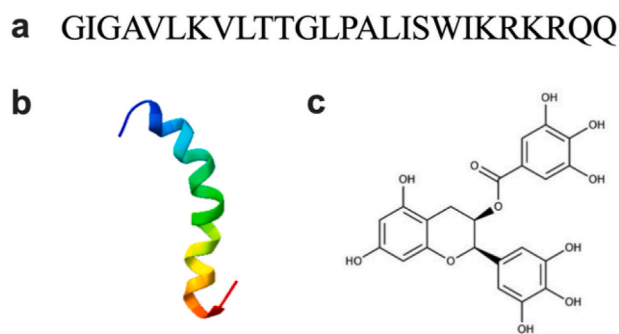


Fig. 1. Sequence and structure of melittin and EGCG. (a) Amino acid sequence of melittin. (b) α -Helical structure of recombinant melittin in an environment that induces the formation of secondary structure (PBD: 6DST). (c) Chemical structure of epigallocatechin gallate (EGCG).

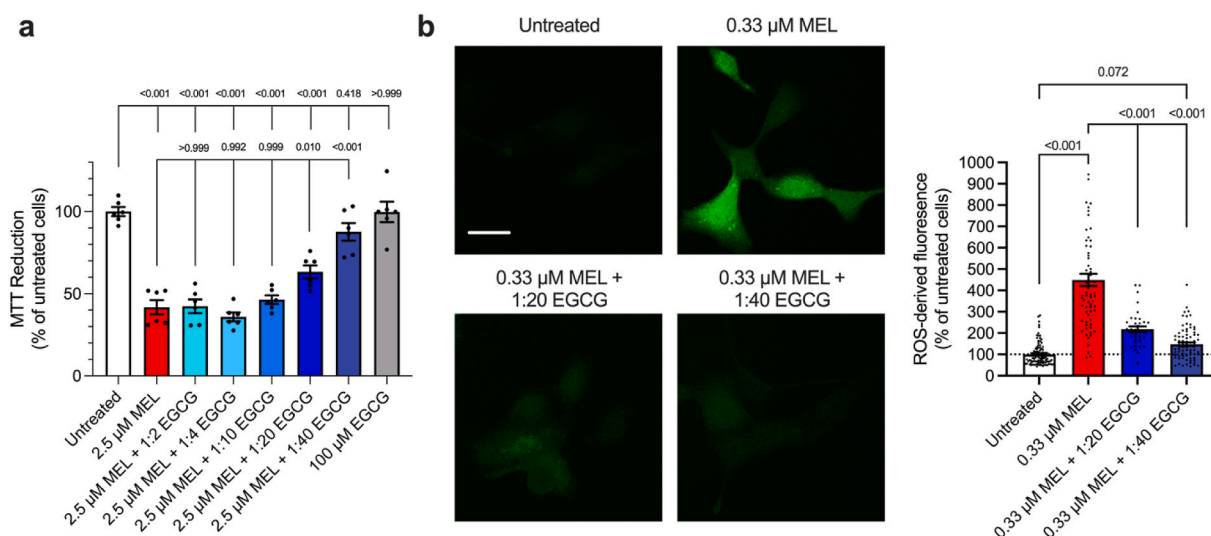


Fig. 2. The cytotoxicity induced by the pore-forming peptide melittin is attenuated by EGCG. (a) MTT viability assays after SH-SY5Y cells were exposed to 2.5 μ M melittin (MEL) in the absence (red bar) or presence of increasing concentrations of EGCG (blue bars) for 30 min. Solutions of melittin with and without EGCG were incubated for 1 h at 37 $^{\circ}$ C under quiescent conditions prior to their exposure to cells. As control, cells were also exposed to 100 μ M EGCG alone (gray bar). 10,000 cells per data point ($n = 6$). Data are representative of three biologically independent experiments. (b) ROS measurements when 0.33 μ M melittin was incubated with SH-SY5Y cells for 5 min in the absence or presence of two ratios of MEL:EGCG (1:20 and 1:40). Cells treated with 13.33 μ M EGCG in the absence of melittin showed similar levels of ROS compared to untreated cells (Supplementary Fig. 1). The fluorescence of CM-H₂DCFDA, general oxidative stress indicator, was used to measure the extent of ROS production in the various conditions. A superimposition of 1.0 μ m thick sections spanning the height of the entire cell generated the shown representative images. Scale bar, 10 μ m. Corresponding semiquantitative values of green fluorescence are shown. Bars indicate mean \pm standard error of the mean (s.e.m.) of 38–130 cells per condition. Data shown are representative of two biologically independent experiments. In all panels, conditions were analyzed by one-way analysis of variance (ANOVA) followed by Dunnett's multiple comparison test relative to untreated cells or cells treated with melittin, as indicated. Untreated cells and cells treated with 100 μ M EGCG were analyzed by an unpaired, two-tailed Student's *t*-test.

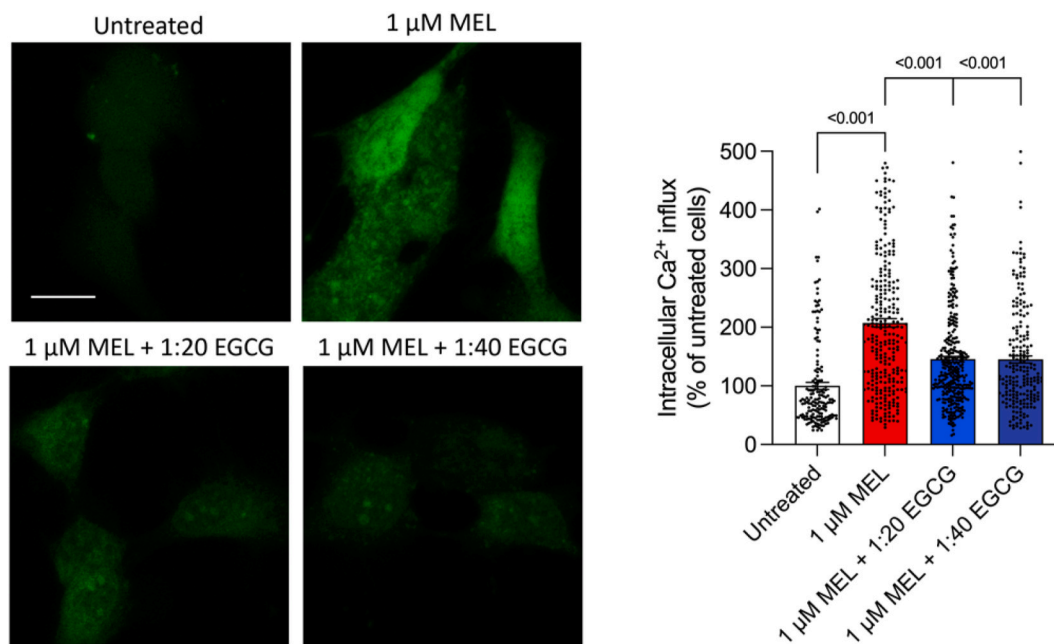


Fig. 3. EGCG attenuates the membrane permeabilizing effect of melittin. Ca²⁺ influx measurements when 1 μ M melittin was incubated with SH-SY5Y cells for 5 min in the absence or presence of two ratios of EGCG (1:20 and 1:40). Solutions of melittin with and without EGCG were incubated for 1 h at 37 $^{\circ}$ C under quiescent conditions prior to their exposure to cells. Cells treated with 40 μ M EGCG in the absence of melittin showed similar levels of Ca²⁺ influx compared to untreated cells (Supplementary Fig. 2). The fluorescence of Fluo-4 AM was used to measure the extent of Ca²⁺ influx in the various conditions. A superimposition of 1.0 μ m thick sections spanning the height of the entire cell generated the shown representative images. Scale bar, 10 μ m. Corresponding semiquantitative values of green fluorescence are shown. Bars indicate mean \pm standard error of the mean (s.e.m.) of at least 150 cells per condition. Data shown are pooled from two biologically independent experiments. Conditions were analyzed by one-way analysis of variance (ANOVA) followed by Dunnett's multiple comparison test or an unpaired, two-tailed Student's *t*-test, as indicated.

1:20 and 1:40 ratios of EGCG. The extent of ROS production was probed using 6-chloromethyl-2',7'-dichlorodihydrofluorescein diacetate (CM-H₂DCFDA) and was quantified using confocal microscopy. Melittin caused a significant increase in ROS production to $449 \pm 5\%$ of untreated cells (mean \pm s.e.m., $p < 0.001$), which was reduced to $217 \pm 13\%$ and $148 \pm 8\%$ of untreated cells for 1:20 and 1:40 ratios of MEL:EGCG, respectively ($p < 0.001$) (Fig. 2b). Cells exposed to the highest concentration of EGCG alone ($13.33 \mu\text{M}$) in the absence of MEL did not exhibit a notable difference in ROS levels from that of untreated cells (Supplementary Fig. 1).

2.2. Melittin induces membrane permeabilization to Ca^{2+} , which is attenuated by EGCG

Past studies have shown that the pore-forming agent melittin is capable of permeabilizing cell membranes [46]. To confirm this effect and the ability of EGCG to protect cell membranes from melittin, we next assessed the rapid influx of Ca^{2+} from cell culture media into the cell following treatment with melittin in the absence or presence of EGCG using Fluo-4 AM, a fluorescent probe that enters cells and produces green fluorescence upon binding to intracellular Ca^{2+} . Ca^{2+} influx following membrane destabilization is thought to be one of the first events in the induction of cytotoxicity, for example upon the exposure of the cells to toxic protein misfolded oligomers of a variety of proteins [47]. Melittin caused a significant increase in Ca^{2+} influx to $207 \pm 7\%$ of

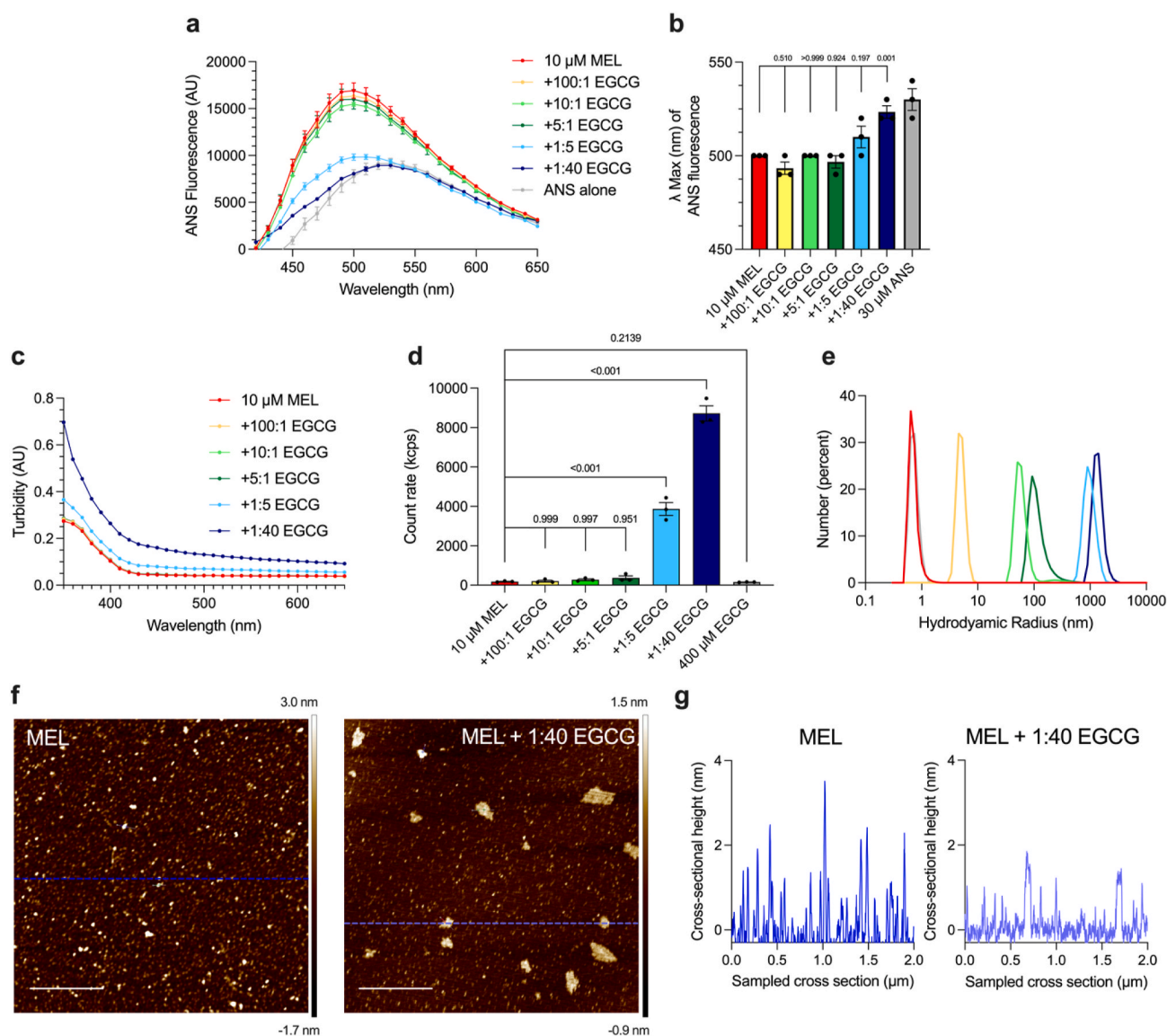


Fig. 4. The physicochemical properties of hydrophobicity and size for melittin are changed by EGCG. (a) 10 μM melittin was incubated for 1 h at room temperature with increasing concentrations of EGCG (MEL:EGCG ratios of 100:1–1:40), after which time 30 μM ANS was added to probe the solvent-exposed hydrophobicity of melittin. Free ANS is shown for reference (gray). Error bars indicate the s.e.m. ($n = 3$). Data shown are representative of four independent experiments. (b) Wavelength of maximum fluorescence (λ_{max}) from (a). Bars indicate mean \pm s.e.m. ($n = 3$). Samples containing melittin and EGCG were analyzed by one-way ANOVA followed by Dunnett's multiple comparison test. (c) Turbidity absorbance measurements for 10 μM melittin incubated with the same conditions shown in (a) ($n = 3$). Data shown are representative of four independent experiments. (d) Static light scattering measurements of the same conditions shown in (a). Bars indicate mean \pm s.e.m. ($n = 3$). Samples containing melittin and EGCG were analyzed by one-way ANOVA followed by Dunnett's multiple comparison test. (e) Dynamic light scattering measurements of the same conditions shown in (a). (f) Melittin was incubated in the absence and presence of a 1:40 ratio of EGCG and measured using atomic force microscopy (AFM). Scale bars, 500 nm. (g) Representative cross-sectional heights are shown, as indicated in the color plots.

untreated cells (mean \pm s.e.m., $p < 0.001$), indicating it strongly increases the permeabilization of SH-SY5Y cells. The extent of Ca^{2+} influx was reduced to $146 \pm 5\%$ and $145 \pm 6\%$ of untreated cells for 1:20 and 1:40 ratios of MEL:EGCG, respectively ($p < 0.001$) (Fig. 3). As control, cells exposed to the highest concentration of EGCG alone ($40 \mu\text{M}$) in the absence of MEL did not exhibit a notable difference in Ca^{2+} levels relative to untreated cells (Supplementary Fig. 2). Overall, the MTT, ROS production, and Ca^{2+} influx assays are in good agreement and indicate that EGCG neutralizes the toxicity of melittin in a dose-dependent manner at super-stoichiometric ratios.

2.3. EGCG decreases the hydrophobicity of melittin

To understand the mechanism by which EGCG attenuates the toxicity of melittin, we next assessed its effect on the solvent-exposed hydrophobicity of melittin using an 8-anilino-1-naphthalenesulfonic acid (ANS) binding assay. $10 \mu\text{M}$ melittin and increasing ratios of EGCG (100:1–1:40 ratios of MEL:EGCG) were probed for solvent-exposed hydrophobicity using ANS. As expected by the fact that melittin has a hydrophobic N-terminal region, we observed that a $10 \mu\text{M}$ concentration of melittin induced a blue shift and increase in fluorescence intensity relative to the unbound dye, indicating the binding of ANS to a solvent-exposed hydrophobic portion of the peptide (Fig. 4a). Higher concentrations of EGCG caused clear decreases in the hydrophobicity of melittin as indicated by the decrease in the intensity of ANS fluorescence of these conditions, until the curve was approximately comparable to that of ANS alone (Fig. 4a). The ANS signal was not overtly changed at the highest concentration of EGCG in the absence of melittin (Supplementary Fig. 3). Typically, a change in protein hydrophobicity is determined through the analysis of the wavelength of maximum ANS fluorescence (λ_{max}), which shifts to blue and red wavelengths upon increasing or decreasing protein solvent-exposed hydrophobicity, respectively. We found that higher ratios of MEL:EGCG (1:5 and 1:40) were necessary to induce a red shift in λ_{max} ($p = 0.197$ and 0.001 , respectively) to the value of ANS alone (Fig. 4b). Across multiple experiments, greater than a 5-fold excess of EGCG was consistently necessary to cause a significant change in λ_{max} under these conditions.

2.4. EGCG increases the size of melittin

To determine the effect of EGCG on the oligomerization of melittin and size of the resulting assemblies, the same samples measured in the ANS assay were also subjected to turbidity absorbance measurements. Similar to the effect seen in ANS experiments, the 1:5 and 1:40 ratios of MEL:EGCG clearly increased the absorbance signal of melittin, indicating an increase in size of particles in solution (Fig. 4c). At the highest concentrations of EGCG alone, small increases in turbidity absorbance were observed. We therefore carried out a subsequent analysis where spectra for EGCG alone were subtracted from the spectra containing MEL and corresponding concentrations of EGCG (Supplementary Fig. 4). Both analyses show that the absorbance of melittin is increased as a function of increasing EGCG concentration.

Static light scattering (SLS) measurements were also carried out at a constant attenuator to further understand the impact of EGCG on the size of melittin in solution in the absence of an additive agent like ANS (Fig. 4d). We found that at the higher ratios of EGCG (1:5 and 1:40), the count rate of scattered photons increased significantly, indicating the presence of larger particles in solution ($p < 0.001$). Subsequently, dynamic light scattering (DLS) measurements were carried out using an automatic attenuator setting. Our DLS experiments showed that as the ratio of EGCG to melittin increased, the hydrodynamic radius of the aggregates in solution increased (Fig. 4e). With $400 \mu\text{M}$ EGCG alone (the highest concentration of EGCG used corresponding to the 1:40 ratio), the size of the particles in solution were similar to the those observed with melittin alone, which excludes the effect of EGCG alone on the observed size increase of melittin in the samples containing both EGCG

and melittin (Supplementary Fig. 5).

We also performed atomic force microscopy (AFM) measurements of $10 \mu\text{M}$ melittin in the absence and presence of a 1:40 ratio of MEL:EGCG (Fig. 4f). The majority of the AFM peaks for melittin alone indicate a height of ca. 1 nm, in agreement with the expected size of monomeric melittin [31] and with the value measured for melittin without EGCG in our DLS measurements. In agreement with the turbidity, SLS, and DLS data, we observed the appearance by AFM of markedly larger and distended aggregates for melittin in the presence of a 40-fold excess of EGCG (Fig. 4g). Collectively, our data support that EGCG induces a dose-dependent increase in the size of melittin, which can be rationalized by the formation of clusters of melittin in solution at higher ratios of EGCG. In such clusters, the majority of the solvent exposed patches are sequestered in the interior of the species, therein rationalizing the reduction in ANS binding.

2.5. EGCG does not impact the secondary structure of melittin

We next sought to measure the secondary structure of melittin upon its EGCG-induced clustering. Circular dichroism (CD) spectroscopy was conducted using $10 \mu\text{M}$ melittin in the absence and presence of 5:1 to 1:5 ratios of MEL:EGCG. The far-UV CD spectrum of melittin demonstrated a minimum at 205 nm and a shoulder near 215–230 nm, indicative of a largely unstructured peptide in solution with residual secondary structures. The melittin spectrum was largely unchanged in the presence of increasing concentrations of EGCG (Fig. 5a). β structure selection (BeStSel) analysis [48,49] of the spectra corroborated that the secondary structure composition of melittin was largely unchanged in the presence of increasing concentrations of EGCG (Fig. 5b). Two-way ANOVA analysis found no significant differences between the secondary structure compositions of melittin alone and any of the samples of melittin with varying concentrations of EGCG. Greater than $50 \mu\text{M}$ concentrations of EGCG were not tested in the CD measurements, as the mean residue ellipticity fluctuated greatly above this concentration, even in the absence of MEL, indicating a high optical absorption of the compound at these high concentrations and interference with CD signal.

2.6. EGCG attenuates the binding of melittin to cell membranes

We next explored the mechanism by which EGCG attenuates the toxicity of melittin to SH-SY5Y cells. It has previously been shown that the binding of misfolded protein oligomers to cell membranes is directly related to toxicity [50]. To determine the extent of the interaction of melittin with cell membranes, we labeled melittin with an Alexa Fluor 488 NHS ester (A488). Adherent SH-SY5Y cells were treated for 5 min at 37°C with $0.33 \mu\text{M}$ A488-labeled melittin in the absence or presence of varying concentrations of EGCG, after which time cells were counterstained with Alexa Fluor 633-conjugated wheat germ agglutinin (WGA, to visualize cell membranes) and fixed.

A488-MEL bound extensively to the cell membrane, as indicated by the green fluorescence of the probe (Fig. 6). The extent of melittin binding was visualized at the apical and medial planes to determine the distribution of melittin on the exterior of the cell membrane and interior of the cell, respectively. Melittin was readily observed in the apical and medial planes of the cell, indicating that it not only binds to the cell membrane, but also enters the cell. Relative to the condition incubated with melittin alone, the addition of a 1:10 ratio of EGCG reduced melittin binding to cell membranes to $61 \pm 2\%$ ($p < 0.001$), and the addition of a 1:40 ratio of EGCG reduced melittin binding to $46 \pm 1\%$ ($p < 0.001$) (Fig. 6). The 1:2 ratio of melittin to EGCG did not cause a significant change in the binding of melittin to the cell membrane ($p = 0.998$). The extent of melittin binding correlates very well with the cell viability data, because both the binding and toxicity of melittin are decreased in a dose-dependent manner upon the addition of increasing concentrations of EGCG.

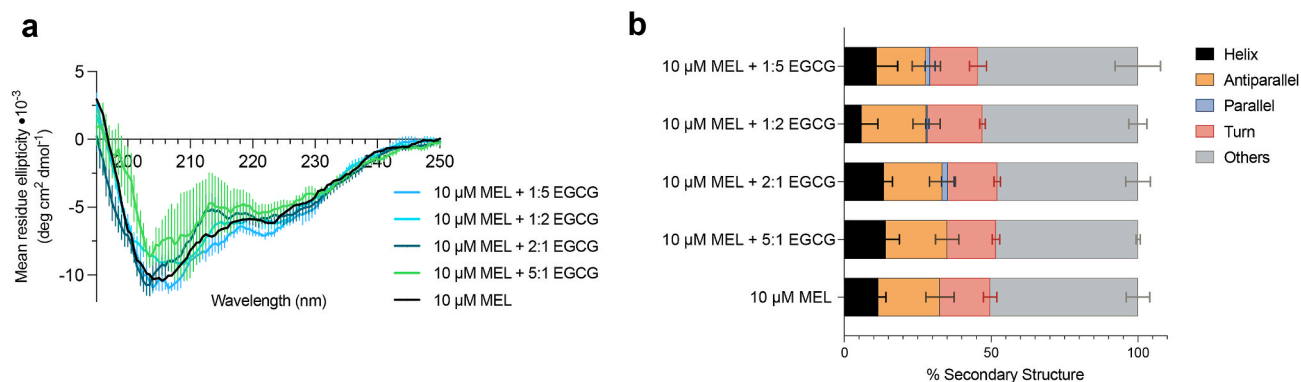


Fig. 5. Secondary structure analysis of melittin with increasing concentrations of EGCG. (a) Far-UV CD spectra for 10 μM melittin in the absence (black trace) and presence of up to a 5-fold excess concentration of EGCG (blue and green traces). Smoothed data are shown. (b) BeStSel-quantified secondary structures for the traces shown in (a). Statistically significant differences were not observed for the samples containing EGCG relative to melittin alone ($p > 0.999$ by two-way ANOVA, main row effect).

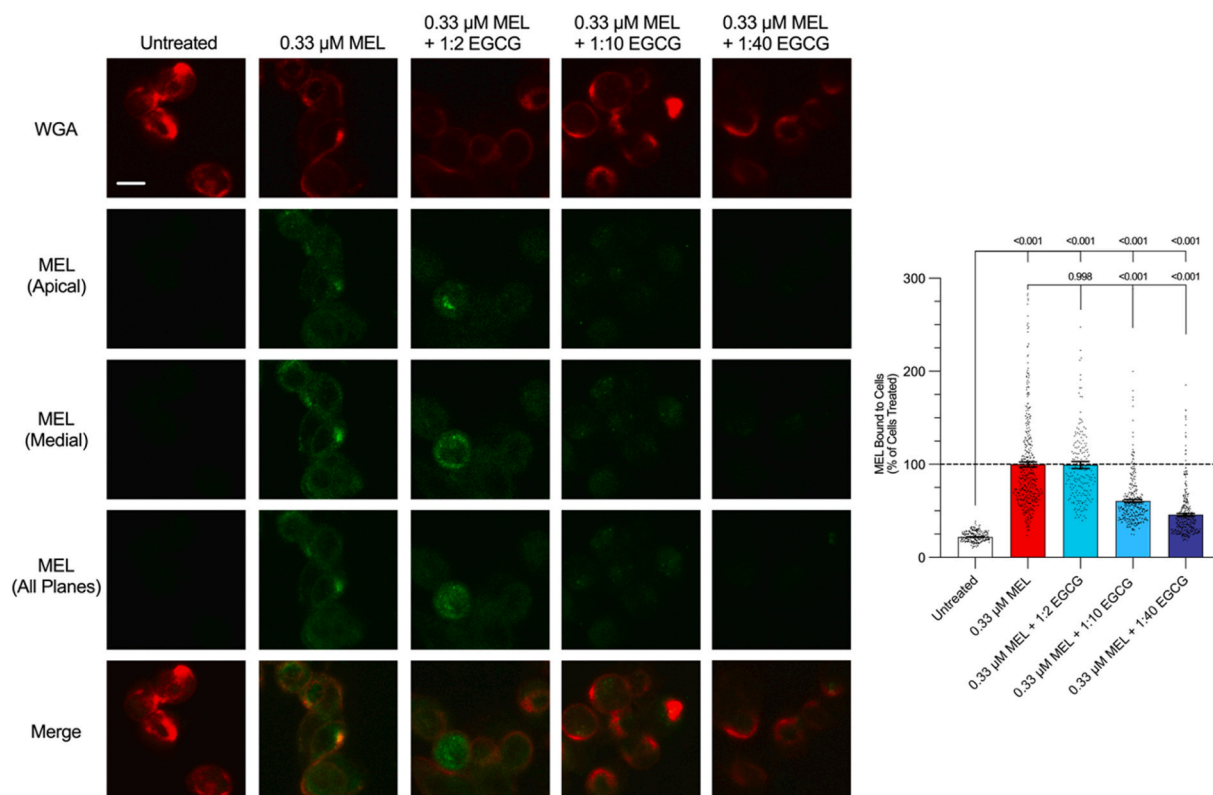


Fig. 6. EGCG attenuates the binding of melittin to cell membranes. Representative images and semi-quantitative bar plot of SH-SY5Y cells treated for 5 min with 0.33 μM melittin (MEL) in the absence (red bar) or presence of 1:2, 1:10, and 1:40 ratios of MEL:EGCG (blue bars). Solutions of melittin with and without EGCG were incubated for 1 h at 37 $^{\circ}\text{C}$ under quiescent conditions prior to their exposure to cells. Untreated cells exposed only to cell culture media are shown for comparison (white bar). In the images, red and green fluorescence correspond to the cell membrane labeled with wheat germ agglutinin (WGA) and A488-labeled melittin, respectively. The apical row corresponds to melittin bound to the exterior of the cell membrane. The medial row corresponds to melittin internalized into the cytosol of the cell. A superimposition of 1.0 μm thick sections spanning the height of the entire cell generated the all planes row. Scale bar, 10 μm . The bar plot shows the colocalization of melittin with the cell membrane. All samples were analyzed by one-way ANOVA followed by Dunnett's multiple comparison test relative to untreated cells. Samples containing melittin and EGCG were analyzed by one-way ANOVA followed by Dunnett's multiple comparison test relative cells treated with melittin alone. Bars indicate mean \pm s.e.m. of at least 190 cells per condition. Data shown are representative of two biologically independent experiments.

2.7. Validation of the clustering-based mechanism by skipping the 1 h EGCG-melittin incubation step

We next conducted MTT cell viability assays without the 1 h incubation of melittin with EGCG at 37 $^{\circ}\text{C}$ under quiescent conditions. Based on our model, the protective effects of EGCG under these conditions is expected to be diminished, because melittin can interact with the cell

membrane without having its physicochemical properties changed by a 1 h interaction with EGCG. SH-SY5Y were treated as before with melittin in the absence and presence of EGCG (1:10 to 1:40 ratios of MEL:EGCG), except the cells were exposed to these solutions immediately upon their formulation. As predicted, the ability of EGCG to neutralize the toxicity of melittin was clearly weakened by a factor of approximately 3.5 at a 40-fold excess concentration of EGCG (Supplementary Fig. 6a) relative

to the case with the incubation step (Fig. 2a). We also found that the hydrophobicity and size of melittin were less changed in the absence of the pre-incubation step. Specifically, the hydrophobicity of melittin was not significantly changed by EGCG under these conditions, as assessed by λ_{max} of ANS fluorescence (Supplementary Figs. 6b and c), and the increase in size of the melittin-EGCG species was clearly reduced, as assessed by both turbidity absorbance (Supplementary Fig. 6d) and dynamic light scattering measurements (Supplementary Fig. 6e) relative to the case with the incubation step (Fig. 4). These results add evidence for the proposed mechanism of action, and illustrate that the formation of the MEL-EGCG clusters is not instantaneous.

2.8. EGCG also neutralizes the toxicity of α -hemolysin

We next sought to determine if the protective effects of EGCG extend to another pore-forming protein that interacts with the cell membrane through a different mechanism. We used α -hemolysin, which is a significantly larger pore-forming protein produced by *Staphylococcus aureus* [51,52]. It has a molecular weight of 33.2 kDa in its monomeric form and 232.4 kDa in its homo-heptameric, β -barrel form that can puncture the cell membrane [51]. The heptamer pore in the cell membrane is large enough to cause the aberrant passage of small molecules

and ions across the cell membrane [53].

We incubated SH-SY5Y cells with 50 μ g/mL (corresponding to approximately 1.5 μ M, in monomer equivalents) α -hemolysin in the absence or presence of increasing concentrations of EGCG for 30 min. Cells were analyzed using the MTT assay in the same manner as conducted in the melittin experiments with the 1 hr incubation step. Similar to the case with melittin, the toxicity of α -hemolysin was significantly decreased in a dose-dependent manner upon the addition of increasing concentrations of EGCG (Fig. 7). α -Hemolysin alone decreased cell viability to $54 \pm 1\%$, whereas the addition of 100 μ M EGCG increased cell viability to $73 \pm 3\%$ ($p < 0.001$) (Fig. 7). Although EGCG was found less protective against α -hemolysin than MEL (compare Figs. 2a and 7), these results indicate that the decrease in toxicity caused by EGCG is not specific to only melittin and may extend to other PFTs and biological threat agents that act by dysregulating the cell membrane.

3. Discussion

The findings that we have reported support the conclusion that EGCG binds to melittin in a manner that induces the creation of larger, less hydrophobic clusters in a dose-dependent fashion, as seen in the ANS and complementary sizing techniques. The EGCG-induced modulation of these physicochemical properties for melittin rationalizes the observed suppression of its membrane affinity and cytotoxicity (Fig. 8), preventing its disruption of the integrity of the membrane and preserving homeostasis within the cell.

Considering that the hydrophobicity of melittin was significantly reduced at greater than a 5-fold excess of EGCG (as seen in the ANS binding assay results), and that its size was significantly increased beginning at a 5-fold excess of EGCG (as seen in the turbidity and SLS results), these data suggest that while the increase in size and decrease in hydrophobicity both contribute to the observed changes in cytotoxicity, a minimum threshold concentration appears to exist for these physicochemical changes to translate to a biological effect. Indeed, cell viability changes were not evident until higher super-stoichiometric ratios of EGCG were used; in particular, a 1:20 ratio of MEL:EGCG was necessary to cause a significant change in cell health relative to the condition in the absence of EGCG in both the MTT, ROS, and Ca^{2+} influx experiments. This is likely a result of insufficient sequestration of the highly cytotoxic melittin at ratios of EGCG below a 20-fold excess to adequately attenuate its toxicity towards neuronal cells. Indeed, our melittin-membrane binding data support the conclusion that clusters of melittin of intermediate size and hydrophobicity are still membrane active and toxic until their hydrophobicity and size are both adequately decreased and increased, respectively.

An increase in Ca^{2+} and ROS levels was clearly observed when cells were exposed to melittin. The apical and medial planes of the binding experiments showed that melittin binds to the cell membrane and enters the cell, respectively. For all these experiments, a treatment time of 5 min was used. This suggests that melittin stresses the cell by both disrupting the cell membrane leading to ion dyshomeostasis, as well as by interacting with endogenous structures in the cytosol, such as the mitochondrial membrane, and cause an increase in ROS production within the cell. The attenuation of membrane-melittin binding caused by EGCG suggests that by changing the physicochemical properties of melittin, EGCG prevents melittin from binding to the cell membrane, forming transmembrane pores, and entering the cell.

The intrinsic anti-inflammatory and antioxidant properties of EGCG [39–42] suggest that it has the potential to improve cell viability in ROS or MTT experiments through a separate mechanism from the direct neutralization of melittin. While we cannot exclude a contribution from the antioxidant effects of EGCG, its impact was limited through short treatment times, specifically 30 min for the MTT assay and 5 min for the Ca^{2+} and ROS assays. Indeed, in both viability assays, a difference was not appreciated between the viability of the untreated cells and those treated with EGCG alone.

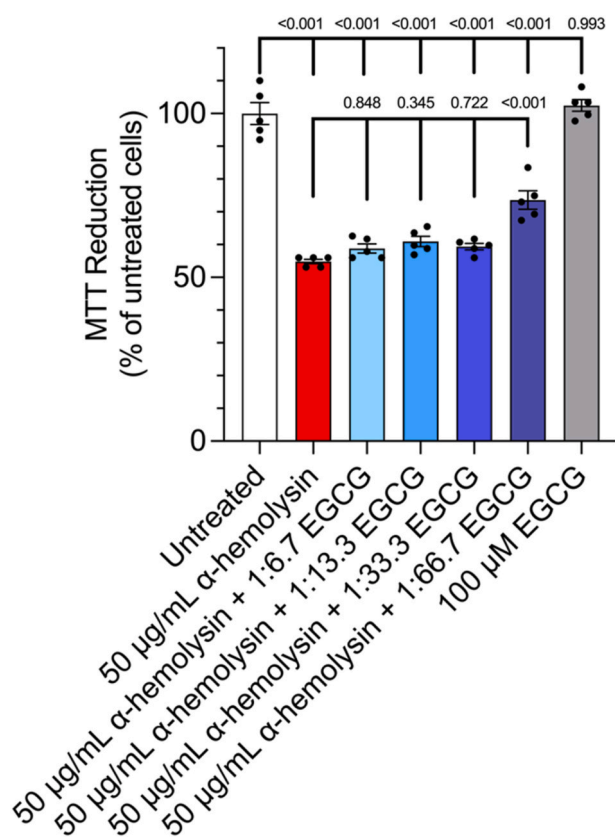


Fig. 7. The cytotoxicity induced by the pore-forming protein α -hemolysin is attenuated by EGCG. MTT viability assay after cells were exposed to 50 μ g/mL α -hemolysin for 30 min in the absence (red) or presence of increasing concentrations of EGCG ranging from 10 to 100 μ M (molar ratios of 1:6.7 to 1:66.7, represented with various blue colors). Solutions of α -hemolysin with and without EGCG were incubated for 1 h at 37 $^{\circ}$ C under quiescent conditions prior to their exposure to cells. As control, cells were also exposed to 100 μ M EGCG alone (gray). $n = 10,000$ cells per data point ($n = 5$). Conditions were analyzed by one-way ANOVA followed by Dunnett's multiple comparison test relative to untreated cells or cells treated with α -hemolysin, as indicated. Untreated cells and cells treated with 100 μ M EGCG were analyzed by an unpaired, two-tailed Student's t -test. Data shown are representative of two biologically independent experiments.

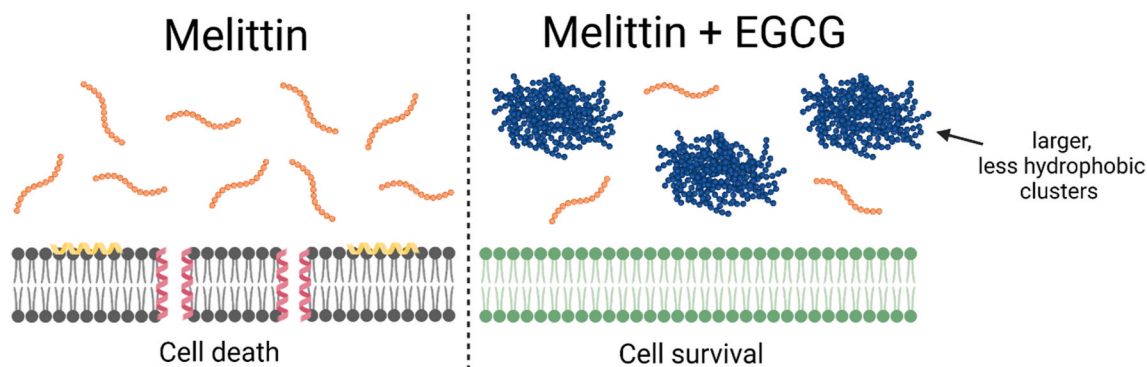


Fig. 8. Schematic for the mechanism by which the toxin melittin disrupts cell membranes and creates pores. Melittin (orange) binds the cell membrane in either a parallel (yellow) or perpendicular (pink) orientation, the latter of which leads to pore formation [26] and ultimately cell death. EGCG causes melittin to clump into larger, less hydrophobic clusters (blue) that show attenuated binding to the cell membrane and, consequently, reduced cytotoxicity. Figure created with biorender.com.

Our results suggest that similar properties can control PFT cytotoxicity in comparison to neurodegenerative diseases. In the context of protein misfolding diseases, the binding affinity of oligomers to the cell membrane is an important initiator of cellular stress through diverse actions on cellular receptors and intracellular targets [2,50]. For misfolded protein oligomers, a clear correlation between the fraction of oligomers bound to the membrane and the resulting cytotoxicity has been established [50,54]. Our results also demonstrate the existence of a similar relationship between the binding affinity of melittin and cellular stress, as increased melittin binding correlated directly with decreased cell health as quantified by the ROS, Ca^{2+} and MTT assays. Furthermore, the relationship between key physicochemical properties and cytotoxicity investigated herein resembles the relationship previously established in studies on misfolded oligomers, where an increase in size and decrease in solvent-exposed hydrophobicity were also directly linked to decreased cytotoxicity [14].

Various small molecules, antibodies, and other molecular species can reduce the toxicity of oligomers associated with neurodegenerative diseases by changing their physicochemical properties and shifting the aggregation of the misfolded protein away from the oligomeric state [55]. One of these compounds is EGCG, which can suppress toxic oligomer formation by binding to natively unfolded monomers of amyloid- β and α -synuclein to prevent amyloid aggregation, by promoting formation of nontoxic oligomers with buried hydrophobic groups or by remodeling mature amyloid fibrils into larger, nontoxic aggregates [47, 56–61]. In tandem with our results herein, these studies collectively raise the possibility that compounds with mechanisms of action similar to that of EGCG could work to neutralize other protein-based biological threat agents through modulating the physicochemical properties responsible for their deleterious membrane interactions.

In a series of related studies, we have previously shown that the aminosterol claramine protects the cell from PFTs without changing the physicochemical properties of these toxins, and instead functions by modulating the properties of the cell membrane to prevent the membrane-toxin interaction [31]. Other aminosterols, squalamine and trodusquemine, have been shown to protect cells from misfolded oligomers associated with Alzheimer's and Parkinson's diseases by an analogous mechanism [54,62–66]. The findings of this study suggest a new approach to protect the cell from PFTs that focuses on modulating the physicochemical properties of the toxins directly, rather than protecting the cell membrane from their action.

4. Conclusions

In summary, claramine and EGCG highlight two different mechanisms of lowering the cytotoxicity of pore-forming toxins (PFTs). The first is binding to cell membranes and protecting them from the

interaction with PFTs, and the second is binding to the PFTs and causing their oligomerization and hydrophobic collapse so that, again, they cannot interact with cell membranes. These results suggest the possibility of developing multiple therapeutic strategies in the protection of cell membranes from a variety of toxins. The results on EGCG, in particular, add further support the notion that the physicochemical properties of biological threat agents impact their ability to bind cell membranes and induce cell death. Overall, our study highlights the importance of physicochemical properties in regulating protein-membrane interactions with shared features between misfolded protein oligomers and non-amyloid forming PFTs, and suggest possible pharmacological approaches based on rational small molecule-protein interactions to neutralize biological toxins.

5. Methods

Reagents. EGCG (at least 95% purity) was acquired from Sigma-Aldrich (MO, USA). Aliquots were prepared at a concentration of 1 mM in water and stored at $-20\text{ }^{\circ}\text{C}$. Melittin (at least 85% purity) was acquired from Sigma-Aldrich (MO, USA) and aliquots were prepared at a concentration of 1 mM in water and stored at $-20\text{ }^{\circ}\text{C}$. α -Hemolysin (>60% protein by Lowry, $\geq 10,000$ units/mg protein) was acquired from Sigma-Aldrich (MO, USA), and aliquots were prepared at a concentration of 500 $\mu\text{g}/\text{mL}$ in water and stored at $-20\text{ }^{\circ}\text{C}$. Samples containing pore-forming agents were handled and disposed of with care and according to the manufacturer's recommendations and guidelines. All samples containing proteins were prepared or stored in Eppendorf LoBind Tubes (Hamburg, Germany).

Neuroblastoma cell culture. Human SH-SY5Y neuroblastoma cells (ATCC, VA, USA) were cultured in DMEM/F-12 with L-glutamine, HEPES, and Phenol Red (11330032, ThermoFisher Gibco, MA, USA) and supplemented with 10% FBS and 1.0% antibiotics (Penicillin-Streptomycin, ThermoFisher Gibco, MA, USA). Cell cultures were maintained in a 5% CO_2 humidified atmosphere at $37\text{ }^{\circ}\text{C}$ and grown until they reached 80% confluence for a maximum of 20 passages [62,67]. The cell line was authenticated and tested negative for mycoplasma contamination.

MTT reduction assay. Melittin (2.5 μM , in monomer equivalents) was added to cell culture medium in the absence of cells and incubated with or without increasing concentrations of EGCG for 1 h at $37\text{ }^{\circ}\text{C}$ under quiescent conditions, and then added to SH-SY5Y cells seeded in 96-well plates for 30 min. 3-(4,5-dimethylthiazol-2-yl)-2,5-diphenyltetrazolium bromide (MTT) was purchased from Sigma-Aldrich, MO, USA, and the MTT reduction assay was performed as previously described [68]. In a separate set of experiments, the assay was conducted without the 1 h incubation step of MEL with EGCG to validate the mechanism of action.

Measurement of intracellular ROS. Melittin (0.33 μM , monomer equivalents) was added to the cell culture medium of SH-SY5Y cells

seeded on glass coverslips (Corning BioCoat Poly-D-Lysin/Laminin, NY, USA) for 5 min in the absence or presence of 1:20 and 1:40 ratios of EGCG. Solutions of melittin with and without EGCG were incubated for 1 h at 37 °C under quiescent conditions prior to their exposure to cells. To detect intracellular ROS production, cells were loaded with 10 µM 6-chloromethyl-2',7'-dichlorodihydrofluorescein diacetate (CM-H₂DCFDA, Life Technologies, CA, USA) during the aforementioned treatment. The resulting fluorescence was analyzed by a Nikon C2 scanning laser confocal microscopy system (Nikon Instruments, NY, USA). A series of 1.0 µm thick optical sections (1024 × 1024) were taken through the cells using a Nikon Eclipse Ti inverted microscope (Nikon Instruments) equipped with a 60× oil immersion objective (Nikon Instruments) and then projected as a single composite image by superimposition. The confocal microscope was set at optimal acquisition conditions, e.g., pinhole diameters, detector gain and laser powers. Settings were maintained constant for all image acquisitions.

Measurement of Ca²⁺ influx. Melittin (1 µM, monomer equivalents) was added to the cell culture medium of SH-SY5Y cells seeded on glass coverslips (Corning BioCoat Poly-D-Lysin/Laminin, NY, USA) for 5 min in the absence or presence of 1:20 and 1:40 ratios of EGCG. Solutions of melittin with and without EGCG were incubated for 1 h at 37 °C under quiescent conditions prior to their exposure to cells. To detect Ca²⁺ influx, cells were then loaded with 10 µM Fluo-4 AM (ThermoFisher Scientific, CA, USA) [47] for 10 min at 37 °C and analyzed using the aforementioned confocal microscopy system, excitation at 488 nm, and overall experimental settings.

Melittin binding to the cellular membrane. To label melittin, 300 µM Alexa Fluor 488 NHS ester (Invitrogen, ThermoFisher Scientific, CA, USA) was incubated with gentle shaking for 2 h with 900 µM melittin in 0.1 mM sodium bicarbonate buffer (pH 8.0, Sigma-Aldrich, MO, USA). It was previously shown that cells exposed to either labeled or unlabeled melittin from 1 to 4 µM exhibited comparable toxicity levels towards SH-SY5Y cells [31]. SH-SY5Y cells were seeded on glass coverslips (Corning BioCoat Poly-D-Lysin/Laminin, NY, USA) and treated for 5 min with 0.33 µM labeled melittin in the absence or presence of 1:2, 1:10, and 1:40 ratios of MEL:EGCG. Samples were prepared as described for the MTT assay. After incubation, the cells were washed with phosphate-buffered saline (PBS) and counterstained with 5 µg/ml Alexa Fluor 633-conjugated wheat germ agglutinin (Life Technologies, CA, USA) [31]. After washing with PBS, cells were fixed in 2% paraformaldehyde. Fluorescence emission was detected after double excitation at 488 nm and 633 nm by the above-described scanning confocal microscopy system using a 60× oil immersion objective (Nikon Instruments). A series of 1.0 µm thick optical sections (1024 × 1024) were acquired and analyzed as indicated. ImageJ (NIH, Bethesda, MD, USA) was used to calculate the percentage of colocalization between cell membranes and melittin.

Circular dichroism spectroscopy. Samples containing 10 µM melittin in the absence and presence of up to 50 µM EGCG were prepared in 20 mM sodium phosphate buffer, pH 7.4. The samples were placed in a clean 1 mm macro cell 110-QS quartz cell and measurements were obtained using a Jasco J-810 CD spectropolarimeter. Scans were acquired in 25 °C, 50 nm/min, over 20 accumulations with a data pitch of 0.5 nm. Data was blank subtracted and normalized to mean residual ellipticity. The BeStSel model [48,49] was used to quantify secondary structure of MEL.

ANS binding measurements. Solutions with melittin (10 µM) in Dulbecco's phosphate-buffered saline (DPBS) were aliquoted after incubation for 1 h at room temperature in the absence or presence of EGCG up to 400 µM, and 30 µM 8-anilino-1-naphthalene-sulfonate (ANS, Sigma-Aldrich, MO, USA) was subsequently added from a 1.5 mM concentrated stock. Emission spectra were recorded using a plate reader (BioTek Synergy H1, VT, USA) with excitation at 380 nm. Spectra were background subtracted to the buffer alone. In a separate set of experiments, the assay was conducted without the 1 h incubation step of MEL with EGCG to validate the mechanism of action.

Turbidity measurements. Samples from the ANS preparation were analyzed for absorbance using a plate reader (BioTek Synergy H1, VT, USA) with spectral scanning. Spectra were acquired from 350 to 650 nm. All traces were background subtracted against buffer alone or to corresponding concentrations of EGCG, as indicated in the text. In a separate set of experiments, the assay was conducted without the 1 h incubation step of MEL with EGCG to validate the mechanism of action.

Static light scattering. Solutions with melittin (10 µM) in DPBS were aliquoted after incubation for 1 h at room temperature in the absence or presence of EGCG up to 400 µM. Static light scattering measurements were performed with fixed parameters for attenuator (11), as determined from the sample of melittin, and cell position of 4.65 mm at 25 °C using the Malvern Zetasizer Nano S instrument (Malvern Panalytical Ltd, Malvern, UK). A low volume (70 µL) disposable cuvette was used (BRAND, Wertheim, Germany).

Dynamic light scattering. Dynamic light scattering was performed using the same materials and conditions described for static light scattering measurements, but with automatic settings for the attenuator and cell position for each sample. In a separate set of experiments, the assay was conducted without the 1 h incubation step of MEL with EGCG to validate the mechanism of action.

Atomic force microscopy (AFM) of melittin. Samples were prepared as described above. AFM sample deposition was carried out at room temperature by depositing a 10 µL drop of protein at a concentration of 10 µM in the absence and presence of a 1:40 ratio of EGCG for 2 min to a freshly cleaved mica surface (AGF7013, Agar Scientific, Essex, United Kingdom). Salt was washed with high purity water and the surface was dried with a gentle stream of nitrogen gas. Samples were stored in a sealed container until imaging using a Bruker Multimode 8 AFM (MA, USA) using tapping mode with scan rates <0.5 Hz and a silicon tip with an 8 nm nominal radius (Model RSTEP, MPP-11100, Bruker, MA, USA). Positively charged melittin in DPBS at pH 7.0–7.3 was easily absorbed to the negatively charged mica substrate without the need for functionalizing the mica substrate and unbound EGCG was washed away during the water rinses.

Statistics. Data were analyzed using GraphPad Prism 9 (CA, USA) using unpaired, two-tailed Student's *t*-tests, two-way ANOVAs, or one-way ANOVAs followed by Dunnett's post comparison test relative to untreated cells or samples containing pore-forming peptides, as indicated in the corresponding figure legends.

Author contributions

J.M.G., D.J.R., S.E., F.C., M.V., and R.L. designed research. J.M.G., T.T., D.J.R., C.M.H., C.J.B., M.G., A.K., T.L.M., M.P., S.C., A.K.W., and R.L. performed research. J.M.G., D.J.R., F.C., M.V. and R.L. analyzed data. J.M.G. and R.L. wrote the original draft. J.M.G. and R.L. conceived the idea for the study. R.L. supervised the study. All authors were involved in the editing of the paper and approved its submission.

Data availability

Data will be made available on request.

Acknowledgements

This research was supported by DTRA Service Academy Research Initiative grants (R.L.), DEVCOM Army Research Laboratory grants (R.L.), the Centre for Misfolding Diseases (D.J.R., S.E. and M.V.), the Gates Cambridge Trust (D.J.R.), Funds RICATEN from the University of Florence (S.E. and F.C.) and the Stamps Scholarship (J.M.G., T.L.M. and S.C.).

Appendix A. Supplementary data

Supplementary data to this article can be found online at <https://doi.org/10.1016/j.cbi.2023.110307>.

org/10.1016/j.cbi.2022.110307.

References

- [1] C. Dias, J. Nylandsted, Plasma membrane integrity in health and disease: significance and therapeutic potential, *Cell Discov* 7 (2021) 4.
- [2] F. Chiti, C.M. Dobson, Protein misfolding, amyloid formation, and human disease: a summary of progress over the last decade, *Annu. Rev. Biochem.* 86 (2017) 27–68.
- [3] M.D. Peraro, F.G. van der Goot, Pore-forming toxins: ancient, but never really out of fashion, *Nat. Rev. Microbiol.* 14 (2016) 77–92.
- [4] A. Halder, S. Karmakar, An evidence of pores in phospholipid membrane induced by an antimicrobial peptide NK-2, *Biophys. Chem.* 282 (2022), 106759.
- [5] M. Pohanka, Current trends in the biosensors for biological warfare agents assay, *Materials* 12 (2019) 2303.
- [6] **Biological agents - overview. Occupational safety and health administration.** <https://www.osha.gov/biological-agents>. (Accessed 3 August 2022).
- [7] C. Lesieur, B. Vécsey-Semjén, L. Abrami, M. Fivaz, F. Gisou van der Goot, Membrane insertion: the strategies of toxins (review), *Mol. Membr. Biol.* 14 (1997) 45–64.
- [8] I. Iacovache, M. Bischofberger, F.G. van der Goot, Structure and assembly of pore-forming proteins, *Curr. Opin. Struct. Biol.* 20 (2010) 241–246.
- [9] E. Gouaux, Channel-forming toxins: tales of transformation, *Curr. Opin. Struct. Biol.* 7 (1997) 566–573.
- [10] F.C.O. Los, T.M. Randis, A.J. Ratner, Role of pore-forming toxins in bacterial infectious diseases, *Microbiol. Mol. Biol. Rev.* 77 (2013) 2.
- [11] S. Karantzoulis, J.E. Galvin, Distinguishing Alzheimer's disease from other major forms of dementia, *Expert Rev. Neurother.* 11 (2011) 1579–1591.
- [12] A.J. Dear, et al., Kinetic diversity of amyloid oligomers, *Proc. Natl. Acad. Sci. U.S.A.* 117 (2020) 12087–12094.
- [13] U. Sengupta, A.N. Nilson, R. Kaye, The role of amyloid- β oligomers in toxicity, propagation, and immunotherapy, *EBioMedicine* 6 (2016) 42–49.
- [14] B. Mannini, et al., Toxicity of protein oligomers is rationalized by a function combining size and surface hydrophobicity, *ACS Chem. Biol.* 9 (2014) 2309–2317.
- [15] P. Cizas, et al., Size-dependent neurotoxicity of β -amyloid oligomers, *Arch. Biochem. Biophys.* 496 (2010) 84–92.
- [16] B. Mannini, et al., Molecular mechanisms used by chaperones to reduce the toxicity of aberrant protein oligomers, *Proc. Natl. Acad. Sci. U.S.A.* 109 (2012) 12479–12484.
- [17] R. Cascella, et al., Transthyretin suppresses the toxicity of oligomers formed by misfolded proteins in vitro, *Biochim. Biophys. Acta BBA - Mol. Basis Dis.* 1832 (2013) 2302–2314.
- [18] B. Mannini, F. Chiti, Chaperones as suppressors of protein misfolded oligomer toxicity, *Front. Mol. Neurosci.* 10 (2017).
- [19] C.R. Dawson, A.F. Drake, J. Helliwell, R.C. Hider, The interaction of bee melittin with lipid bilayer membranes, *Biochim. Biophys. Acta BBA - Biomembr.* 510 (1978) 75–86.
- [20] T.C. Terwilliger, L. Weissman, D. Eisenberg, The structure of melittin in the form I crystals and its implication for melittin's lytic and surface activities, *Biophys. J.* 37 (1982) 353–361.
- [21] C.E. Dempsey, The actions of melittin on membranes, *Biochim. Biophys. Acta BBA - Rev. Biomembr.* 1031 (1990) 143–161.
- [22] L. Yang, T.A. Harroun, T.M. Weiss, L. Ding, H.W. Huang, Barrel-stave model or toroidal model? a case study on melittin pores, *Biophys. J.* 81 (2001) 1475–1485.
- [23] M.S. Sansom, The biophysics of peptide models of ion channels, *Prog. Biophys. Mol. Biol.* 55 (1991) 139–235.
- [24] Y. Wu, et al., Permeation of styryl dyes through nanometer-scale pores in membranes, *Biochemistry* 50 (2011) 7493–7502.
- [25] M.-T. Lee, T.-L. Sun, W.-C. Hung, H.W. Huang, Process of inducing pores in membranes by melittin, *Proc. Natl. Acad. Sci. U.S.A.* 110 (2013) 14243–14248.
- [26] G. van den Bogaart, J.V. Guzmán, J.T. Mika, B. Poolman, On the mechanism of pore formation by melittin, *J. Biol. Chem.* 283 (2008) 33854–33857.
- [27] J.H. Choi, et al., Melittin, a honeybee venom-derived antimicrobial peptide, may target methicillin-resistant *Staphylococcus aureus*, *Mol. Med. Rep.* 12 (2015) 6483–6490.
- [28] M.-T. Lee, W.-C. Hung, F.-Y. Chen, H.W. Huang, Mechanism and kinetics of pore formation in membranes by water-soluble amphipathic peptides, *Proc. Natl. Acad. Sci. U.S.A.* 105 (2008) 5087–5092.
- [29] D. Sun, J. Forsman, C.E. Woodward, Multistep molecular dynamics simulations identify the highly cooperative activity of melittin in recognizing and stabilizing membrane pores, *Langmuir* 31 (2015) 9388–9401.
- [30] S.-C. Park, et al., Investigation of toroidal pore and oligomerization by melittin using transmission electron microscopy, *Biochem. Biophys. Res. Commun.* 343 (2006) 222–228.
- [31] R.P. Kreiser, et al., A brain-permeable aminosterol regulates cell membranes to mitigate the toxicity of diverse pore-forming agents, *ACS Chem. Neurosci.* 13 (2022) 1219–1231.
- [32] G.-J. Du, et al., Epigallocatechin gallate (egcg) is the most effective cancer chemopreventive polyphenol in green tea, *Nutrients* 4 (2012) 1679–1691.
- [33] S. Bettuzzi, et al., Chemoprevention of human prostate cancer by oral administration of green tea catechins in volunteers with high-grade prostate intraepithelial neoplasia: a preliminary report from a one-year proof-of-principle study, *Cancer Res.* 66 (2006) 1234–1240.
- [34] S. Zhang, Q. Zhu, J.-Y. Chen, D. OuYang, J.-H. Lu, The pharmacological activity of epigallocatechin-3-gallate (EGCG) on Alzheimer's disease animal model: a systematic review, *Phytomedicine* 79 (2020), 153316.
- [35] J.C. Blackburn, E. Magness, J.L. Roberts, Have some tea, feed your brain: how egcg acts as a protective agent in a parkinsonian model, *Faseb. J.* 32 (2018), lb421–lb421.
- [36] D.G. Raederstorff, M.F. Schlachter, V. Elste, P. Weber, Effect of EGCG on lipid absorption and plasma lipid levels in rats, *J. Nutr. Biochem.* 14 (2003) 326–332.
- [37] S. Wolfram, Effects of green tea and egcg on cardiovascular and metabolic health, *J. Am. Coll. Nutr.* 26 (2007) 373S–388S.
- [38] R. Hursel, W. Viechtbauer, M.S. Westerterp-Plantenga, The effects of green tea on weight loss and weight maintenance: a meta-analysis, *Int. J. Obes.* 33 (2009) 956–961.
- [39] J.V. Higdon, B. Frei, Tea catechins and polyphenols: health effects, metabolism, and antioxidant functions, *Crit. Rev. Food Sci. Nutr.* 43 (2003) 89–143.
- [40] Y. Zhong, F. Shahidi, Lipophilized epigallocatechin gallate (EGCG) derivatives as novel antioxidants, *J. Agric. Food Chem.* 59 (2011) 6526–6533.
- [41] T. Ohishi, S. Goto, P. Monira, M. Isemura, Y. Nakamura, Anti-inflammatory action of green tea, Anti-inflammatory Agents Med. Chem. 15 (2016) 74–90.
- [42] Y. Zhong, C.-M. Ma, F. Shahidi, Antioxidant and antiviral activities of lipophilic epigallocatechin gallate (EGCG) derivatives, *J. Funct. Foods* 4 (2012) 87–93.
- [43] M. Pervin, et al., Blood brain barrier permeability of (–)-epigallocatechin gallate, its proliferation-enhancing activity of human neuroblastoma SH-SY5Y cells, and its preventive effect on age-related cognitive dysfunction in mice, *Biochem. Biophys. Res. Rep.* 9 (2017) 180–186.
- [44] K. Kawaguchi, T. Matsumoto, Y. Kumazawa, Effects of antioxidant polyphenols on tnf-alpha-related diseases, *Curr. Top. Med. Chem.* 11 (2011) 1767–1779.
- [45] I.-B. Kim, et al., Inhibition of IL-8 production by green tea polyphenols in human nasal fibroblasts and A549 epithelial cells, *Biol. Pharm. Bull.* 29 (2006) 1120–1125.
- [46] W.C. Wimley, How does melittin permeabilize membranes? *Biophys. J.* 114 (2018) 251–253.
- [47] R. Cascella, et al., The release of toxic oligomers from α -synuclein fibrils induces dysfunction in neuronal cells, *Nat. Commun.* 12 (2021) 1814.
- [48] A. Micsonai, et al., Accurate secondary structure prediction and fold recognition for circular dichroism spectroscopy, *Proc. Natl. Acad. Sci. U.S.A.* 112 (2015) E3095–E3103.
- [49] A. Micsonai, et al., BeStSel: a web server for accurate protein secondary structure prediction and fold recognition from the circular dichroism spectra, *Nucleic Acids Res.* 46 (2018) W315–W322.
- [50] E. Evangelisti, et al., Binding affinity of amyloid oligomers to cellular membranes is a generic indicator of cellular dysfunction in protein misfolding diseases, *Sci. Rep.* 6 (2016), 32721.
- [51] L. Song, et al., Structure of staphylococcal α -hemolysin, a heptameric transmembrane pore, *Science* 274 (1996) 1859–1865.
- [52] D. Dahlberg, et al., Staphylococcal α -hemolysin is neurotoxic and causes lysis of brain cells in vivo and in vitro, *Neurotoxicology* 48 (2015) 61–67.
- [53] B.J. Berube, J.B. Wardenburg, *Staphylococcus aureus* α -toxin: nearly a century of intrigue, *Toxins* 5 (2013) 1140–1166.
- [54] R. Limbocker, et al., Squalamine and trodusquemine: two natural products for neurodegenerative diseases, from physical chemistry to the clinic, *Nat. Prod. Rep.* 39 (2022) 742–753.
- [55] R.P. Kreiser, et al., Therapeutic strategies to reduce the toxicity of misfolded protein oligomers, *Int. J. Mol. Sci.* 21 (2020) 8651.
- [56] E.Y. Choi, S.S. Kang, S.K. Lee, B.H. Han, Polyphenolic biflavonoids inhibit amyloid-beta fibrillation and disaggregate preformed amyloid-beta fibrils, *Biomol. Ther.* 28 (2020) 145–151.
- [57] S. Giorgetti, C. Greco, P. Tortora, F.A. Aprile, Targeting amyloid aggregation: an overview of strategies and mechanisms, *Int. J. Mol. Sci.* 19 (2018) 2677.
- [58] F.L. Palhano, J. Lee, N.P. Grimster, J.W. Kelly, Toward the molecular mechanism (s) by which egcg treatment remodels mature amyloid fibrils, *J. Am. Chem. Soc.* 135 (2013) 7503–7510.
- [59] J. Bieschke, et al., EGCG remodels mature α -synuclein and amyloid- β fibrils and reduces cellular toxicity, *Proc. Natl. Acad. Sci. U.S.A.* 107 (2010) 7710–7715.
- [60] D.E. Ehrnhoefer, et al., EGCG redirects amyloidogenic polypeptides into unstructured, off-pathway oligomers, *Nat. Struct. Mol. Biol.* 15 (2008) 558–566.
- [61] G. Fusco, et al., Structural basis of membrane disruption and cellular toxicity by α -synuclein oligomers, *Science* 358 (2017) 1440–1443.
- [62] R. Limbocker, et al., Trodusquemine enhances A β 42 aggregation but suppresses its toxicity by displacing oligomers from cell membranes, *Nat. Commun.* 10 (2019) 225.
- [63] R. Limbocker, et al., Trodusquemine displaces protein misfolded oligomers from cell membranes and abrogates their cytotoxicity through a generic mechanism, *Commun. Biol.* 3 (2020) 435.
- [64] R. Limbocker, et al., Squalamine and its derivatives modulate the aggregation of amyloid- β and α -synuclein and suppress the toxicity of their oligomers, *Front. Neurosci.* 15 (2021).
- [65] M. Perni, et al., A natural product inhibits the initiation of α -synuclein aggregation and suppresses its toxicity, *Proc. Natl. Acad. Sci. U.S.A.* 114 (2017) E1009–E1017.
- [66] M. Perni, et al., Multistep inhibition of α -synuclein aggregation and toxicity in vitro and in vivo by trodusquemine, *ACS Chem. Biol.* 13 (2018) 2308–2319.
- [67] R. Cascella, et al., Probing the origin of the toxicity of oligomeric aggregates of α -synuclein with antibodies, *ACS Chem. Biol.* 14 (2019) 1352–1362.
- [68] R. Cascella, et al., Soluble oligomers require a ganglioside to trigger neuronal calcium overload, *J. Alzheimers Dis.* 60 (2017) 923–938.